Run-away Stars

A project for the course of study "Physik mit integriertem Doktorandenkolleg" of the University of Regensburg

by Andreas Irrgang

November 2008

Supervisor: Prof. Dr. Ulrich Heber
Dr. Remeis Observatory Bamberg
Astronomical Institute of the University of Erlangen-Nuremberg

Abstract

Investigations based on kinematic properties are performed for eleven run-away stars in order to find their possible places of birth in the Galactic disk and hence gaining hints of how they could have emerged.

Contents

List of Figures

List of Tables

1 Introduction

According to [11] a run-away star is a "star that is moving with very high velocity, typically hundreds of kilometers per second, relative to the local standard of rest". Up to now, two generally accepted scenarios for its creation exist: firstly, the star is the minor component of a binary systems whose primary star explodes as a supernova enabling the other one to escape from the formerly bound system. Secondly, the run-away star could be produced by close dynamical encounters in dense star clusters such as binary-binary interactions.

Due to their high velocities, run-away stars are able to pass through large regions of the Galaxy and therefore being good probes for the Galactic gravitational potential provided that their ejection mechanism is sufficiently understood. On the other hand, it may be possible to infer information about the complex processes that take place during supernova explosions respectively many-body interactions from the spectroscopic and kinematic properties of these stars. Perhaps one could even gain some hints about regroupment processes that take place at the star's surface when supernova ejecta are brought to deeper layers of its atmosphere.

Usually the ejection velocity of run-away stars is smaller than the Galactic escape speed leading to bound motions of these stars (the only known exception is HD 271791, see [4], which is a particular case). Nevertheless several stars with velocities exceeding the escape speed of the Galaxy are observed, the so-called hyper-velocity stars. It is generally assumed that they are produced by a supermassive black hole in the Galactic center, whose tidal forces might disrupt a closely passing binary system and accelerate one member to sufficient large velocities (see [5]). However, the example of HD 271791 shows that both types are tightly related.

In this project the possible origins in the Galactic disk of eleven run-away stars are examined by numerical means. In order to do so, the three spatial velocity components of each star are derived from their spectroscopic quantities m_{V}, T_{eff}, $\log(\frac{g}{\mathrm{cms}^{-2}})$, v_{rad} and from their proper motions μ_α and μ_δ. Having the current positions and velocities and a model for the gravitational potential of the Galaxy, the stars' orbits are numerically calculated back in time to find the intersection point with the Galactic disk. The stellar region around the intersection point might give hints of how the stars have been produced.

2 Determination of three dimensional velocity components

2.1 Equatorial coordinate system

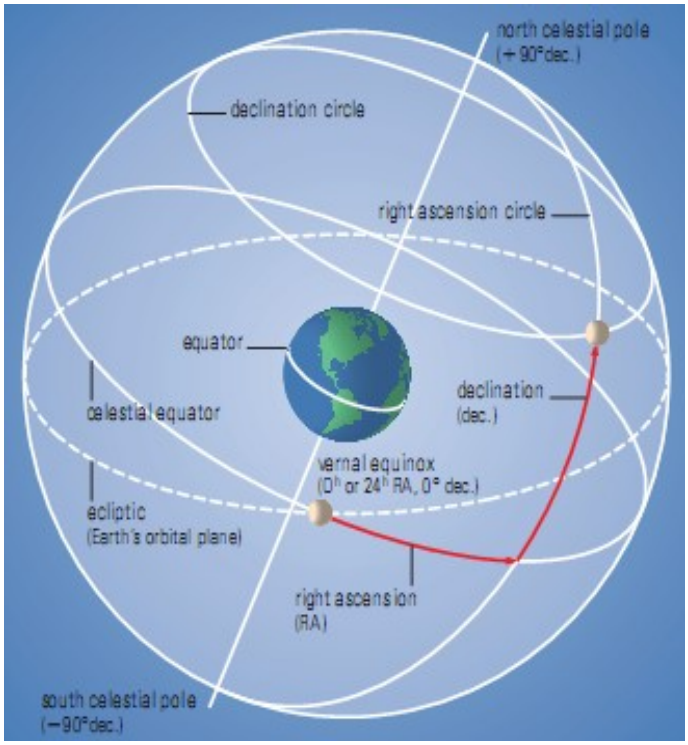

Figure 1: Right ascension α and declination δ in the equatorial system (taken from [10]).

The (almost) constant rotation axis of the Earth provides a quite natural coordinate system for astronomers, namely equatorial coordinates given

by right ascension α and declination δ and using the celestial equator as plane of reference. As illustrated in figure 1 α is measured along the celestial equator in hours, minutes and seconds from the vernal equinox point – the fixed intersection of the celestial equator with the ecliptic occurring in spring – to the object in east direction. Declination is measured from 0° to 90°/-90° between celestial equator and the north/south celestial pole. Tangential velocities are given by proper motions μ_α and μ_δ, which are the angular velocities in α and δ, via $v_\alpha = d{\cdot}\cos(\delta){\cdot}\mu_\alpha$[1] and $v_\delta = d{\cdot}\mu_\delta$ with d being the distance from the object to Earth. Additionally one has the heliocentric radial velocity v_{rad}, corrected for Earth's motion and rotation.

2.2 Obtaining distances from spectroscopy

For all stars, considered in this project, proper motions are available in various astronomical catalogs. But in order to convert them into tangential velocities, the distances d of the respective stellar bodies are needed.

Fitting simulated spectra, numerically computed from theoretical model atmospheres, to measured stellar spectra, it is possible to determine the two quantities $\log(\frac{g}{\text{cms}^{-2}})$ (surface gravity) and T_{eff} (effective temperature: temperature of an object found by assuming that its total emission over all wavelengths is that of a black body). Moreover, again using simulated model atmospheres, one can get the flux $F_{\text{V}}\left(\log(\frac{g}{\text{cms}^{-2}}), T_{\text{eff}}\right)$ (in units of $\frac{\text{erg}}{\text{cm}^2\text{s}\,\mathring{\text{A}}}$) at visual wavelength $\lambda_{\text{V}} = 550\text{nm}$ emanating from the stellar surface for given g and T_{eff} (see [6]). However, since the stellar spectrum is influenced almost solely by the surface of the star, properties like mass or radius are unaccessible via spectroscopy.

Unfortunately mass is necessary to specify the distance: Neglecting interstellar absorption, one has as direct consequence of energy conservation (with f_{V} denoting the flux arriving at Earth again in units of $\frac{\text{erg}}{\text{cm}^2\text{s}\,\mathring{\text{A}}}$ and R_{S} being the star's radius):

$$4\pi {R_{\text{S}}}^2 F_{\text{V}} = 4\pi d^2 f_{\text{V}} \;\Rightarrow\; f_{\text{V}} = \left(\frac{R_{\text{S}}}{d}\right)^2 F_{\text{V}} \quad (2.1)$$

Using Newton's law of gravitation at the surface of the star $g = \frac{GM}{{R_{\text{S}}}^2} \;\Rightarrow\; {R_{\text{S}}}^2 = \frac{GM}{g}$:

$$d = \sqrt{\frac{\text{GM}}{g}\frac{F_{\text{V}}}{f_{\text{V}}}} \quad (2.2)$$

A solution to this problem is given by stellar evolution models based on the following observation: Plotting a $\log(g) - \log(T_{\text{eff}})$ diagram for a large number of stars of the same type and mass with different lifetimes, one recognizes a definite track in the a $\log(g) - \log(T_{\text{eff}})$ plane. These so-called evolution tracks, describing a star's time evolution, depend on the stellar mass and can quite well be reproduced by computer models (see e.g. [15]). Hence mass and evolution age T_{evol} can be derived from the stars' location in the corresponding diagrams, for instance see figure 2:

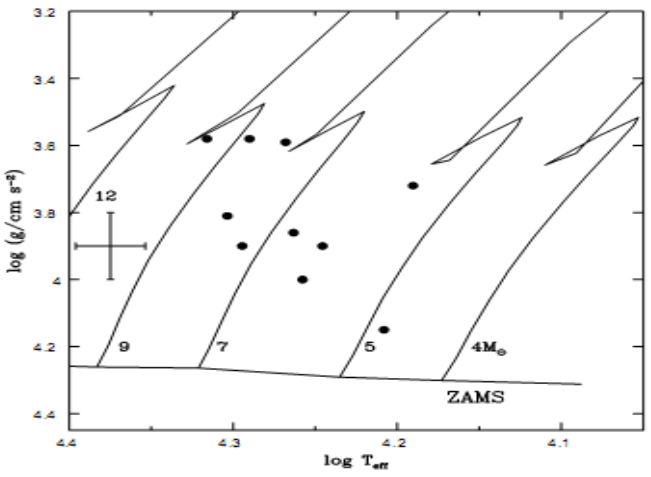

Figure 2: $\log(g) - \log(T_{\text{eff}})$ diagram for different stellar masses: each filled dot represents a star (taken from [13])

The only remaining unknown quantity in equation 2.2 is f_{V}, which is, however, closely related to the visual magnitude m_{V} by definition of the

[1] it is customary in literature to list $\mu_\alpha \cdot \cos(\delta)$ instead of μ_α

latter:

$$m_{\mathrm{V}} = -2.5\log(f_{\mathrm{V}}\frac{\mathrm{cm^2 s\,\mathring{A}}}{\mathrm{erg}}) - 21.107 \qquad (2.3)$$

The last term defines the historically set zero point of the magnitude scale. Solving this for f_{V}:

$$f_{\mathrm{V}} = 3.607\cdot 10^{-9}\frac{\mathrm{erg}}{\mathrm{cm^2 s\,\mathring{A}}}10^{-0.4m_{\mathrm{V}}} \qquad (2.4)$$

Eventually introducing the astrophysical flux $\mathcal{F}_{\mathrm{V}}$ by $F_{\mathrm{V}} = \pi\cdot\mathcal{F}_{\mathrm{V}}$ and inserting everything into equation 2.2, one maintains:

$$d\left(m_{\mathrm{V}}, M, T_{\mathrm{eff}}, \log\left(\frac{g}{\mathrm{cms^{-2}}}\right)\right) = 1.11\mathrm{kpc}\cdot$$
$$\cdot\sqrt{\frac{M}{M_\odot}\frac{\mathrm{cms^{-2}}}{g}\frac{\mathcal{F}_{\mathrm{V}}\left(T_{\mathrm{eff}}, \log\left(\frac{g}{\mathrm{cms^{-2}}}\right)\right)}{10^8\mathrm{ergcm^{-2}s^{-1}\mathring{A}^{-1}}}10^{0.4m_{\mathrm{V}}}} \qquad (2.5)$$

Table 1 lists the distances obtained from the data of table 3 of appendix A, and compares them to values given in literature if available.

Table 1: Distances d of investigated stars: the errors originate from taking a general uncertainty of 0.2 for $\log\left(\frac{g}{\mathrm{cms^{-2}}}\right)$ and neglecting all other errors for quantities occurring in equation 2.5. For comparison, values d_{lit} taken from the corresponding reference are stated as well.

star	d[kpc]	d_{lit}[kpc]	reference
HIP 60350	3.6 ± 0.6	3.5	[7]
PG 0934+145	7 ± 2	-	-
Feige 40	1.3 ± 0.3	1.26	[9]
PG 1205+228	2.4 ± 0.4	2.8	[14]
PG 1315-077	4.2 ± 0.7	-	-
PHL 159	5.4 ± 0.9	5.3	[13]
PHL 346	9 ± 2	8.7	[13]
BD -15 115	4.6 ± 0.8	4.9	[13]
PG 2345+241	4.8 ± 0.8	-	-
HD 149363	1.1 ± 0.2	1.21	[9]
HD 209684	1.7 ± 0.3	1.54	[9]

2.3 Velocity

The three dimensional velocity is finally given by its two tangential components $v_\alpha = d\cdot\cos(\delta)\cdot\mu_\alpha$ and $v_\delta = d\cdot\mu_\delta$, summarized in table 2, and its radial component v_{rad}, gained from the Doppler-shift of atomic line transition wavelengths in the spectra.

Table 2: Tangential velocities $v_\alpha = d\cdot\cos(\delta)\cdot\mu_\alpha$ and $v_\delta = d\cdot\mu_\delta$ of analyzed stars:

star	v_α[km/s]	v_δ[km/s]
HIP 60350	-240 ± 80	280 ± 50
PG 0934+145	230 ± 145	-130 ± 120
Feige 40	-6 ± 14	-42 ± 23
PG 1205+228	-180 ± 60	-7 ± 12
PG 1315-077	-150 ± 160	-50 ± 60
PHL 159	-80 ± 70	-230 ± 70
PHL 346	210 ± 140	-330 ± 120
BD -15 115	170 ± 80	4 ± 14
PG 2345+241	-50 ± 60	-90 ± 60
HD 149363	-47 ± 14	-73 ± 24
HD 209684	0 ± 20	-8 ± 6

3 Galactic gravitational potential

Calculating orbits of stars requires a suitable model for the Galactic gravitational potential, for instance given by Allen & Santillán (see [1]). Using Galactic cylindrical coordinates r, φ and z with $r = z = 0$ corresponding to the Galactic center and the relation $R = \sqrt{r^2 + z^2}$, their potential, consisting of a spherical central mass distribution simulating the bulge $\Phi_{\mathrm{B}}(R)$, a disk component $\Phi_{\mathrm{D}}(r, z)$ and a spherical halo $\Phi_{\mathrm{H}}(R)$, has the simple form:

$$\Phi(r, z) = \Phi_{\mathrm{B}}(r, z) + \Phi_{\mathrm{D}}(r, z) + \Phi_{\mathrm{H}}(r, z) \qquad (3.1a)$$

whereby

$$\Phi_{\mathrm{B}}(r,z) = \Phi_{\mathrm{B}}(R) = -\frac{\mathrm{M_B}}{\sqrt{R^2 + \mathrm{b_B}^2}} \tag{3.1b}$$

$$\Phi_{\mathrm{D}}(r,z) = -\frac{\mathrm{M_D}}{\sqrt{r^2 + \left(\mathrm{a_D} + \sqrt{z^2 + \mathrm{b_D}^2}\right)^2}} \tag{3.1c}$$

$$\Phi_{\mathrm{H}}(r,z) = \Phi_{\mathrm{H}}(R) = -\frac{\mathrm{M_H}\cdot\left(\frac{R}{\mathrm{a_H}}\right)^{2.02}}{\left(1+\left(\frac{R}{\mathrm{a_H}}\right)^{1.02}\right)\cdot R} - \frac{\mathrm{M_H}}{1.02\mathrm{a_H}}\cdot$$
$$\cdot\left[\ln\left(1+\left(\frac{x}{\mathrm{a_H}}\right)^{1.02}\right) - \frac{1.02}{1+\left(\frac{x}{\mathrm{a_H}}\right)^{1.02}}\right]_{x=R}^{x=100\mathrm{kpc}} \tag{3.1d}$$

Giving distances in kpc and masses in terms of Galactic mass $\mathrm{M_{Gal}}$ ($\mathrm{M_{Gal}} = 2.32 \cdot 10^7\ \mathrm{M_\odot}$) the gravitational constant G is unity. The parameters used in the above equations are obtained by fitting the results of computations based on the model potential to observations such as Galactic rotation curve or perpendicular force and are given by: $\mathrm{M_B} = 606.0\ \mathrm{M_{Gal}}$, $\mathrm{M_D} = 3690.0\ \mathrm{M_{Gal}}$, $\mathrm{M_H} = 4615.0\ \mathrm{M_{Gal}}$, $\mathrm{b_B} = 0.3873$ kpc, $\mathrm{a_D} = 5.3178$ kpc, $\mathrm{b_D} = 0.2500$ kpc, $\mathrm{a_H} = 12.0$ kpc.

From the definition of the gravitational potential $\Phi(\vec{x}) = -\mathrm{G}\int_{\mathrm{V}} \frac{\rho(\acute{\vec{x}})}{|\vec{x}-\acute{\vec{x}}|}\mathrm{d}^3\acute{x}$ and the well known identity $\nabla_x^2 \frac{1}{|\vec{x}-\acute{\vec{x}}|} = -4\pi\delta\left(\vec{x}-\acute{\vec{x}}\right)$ one immediately obtains the Poisson equation enabling one to calculate the mass density $\rho(\vec{x})$ from $\Phi(\vec{x})$:

$$\nabla_x^2 \Phi(\vec{x}) = 4\pi\mathrm{G}\rho(\vec{x}) \tag{3.2}$$

The choices made for Φ in equations 3.1b and 3.1c are such, that on the one hand extreme mathematical simplicity is achieved and on the other hand the resulting densities are in good correspondence to the observed mass distribution. E.g. applying the Poisson equation to Φ_{D} in fact yields a disk–like density just as seen in the Milky Way. The form of Φ_{H} in equation 3.1d arises from the following: in order to reproduce the observed flat rotation curve of the Galaxy, the mass of the halo's dark matter, enclosed in a sphere of radius R, has to grow linearly with R at least for large R, for instance $M(R) = \frac{M_{\mathrm{H}}(R/a_{\mathrm{H}})^{2.02}}{1+(R/a_{\mathrm{H}})^{1.02}}$. What is more since the gravitational potential of a homogeneous sphere is equal to that of a point-like mass at its center for the case that one is outside the sphere respectively constant when being inside it, one has:

$$\Phi_{\mathrm{H}}(R) = -\frac{M(R)}{R} - \int_R^{100\mathrm{kpc}} \frac{1}{\acute{R}}\frac{\mathrm{d}M(\acute{R})}{\mathrm{d}\acute{R}}\mathrm{d}\acute{R} \tag{3.3}$$

An arbitrary cutoff for the halo at $R = 100$ kpc has been introduced. Performing the integration with $M(R)$ given above, equation 3.3 becomes 3.1d.

Figure 3 illustrates the resulting mass densities:

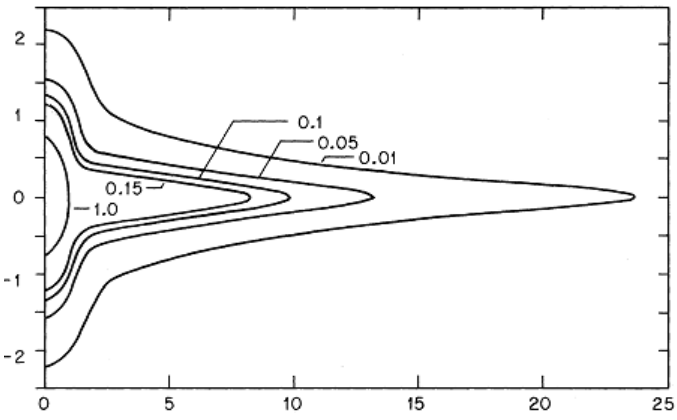

Figure 3: Contours of equal density $\rho(r,z)$ in the r-z plane (units are kpc) obtained from the Allen & Santillán potential described by equations 3.1 (taken from [1]).

Advantages of the Allen & Santillán potential are its closed analytic form, mathematical simplicity, lack of unphysical expressions like negative mass densities and good agreement with observational data.

4 Numerical program and error estimation

Numerical computations are performed with the program ORBIT6 developed by Odenkirchen &

Brosche (see [12]), which calculates the time dependent coordinates and velocities of a test body in the Galactic potential of Allen & Santillán in equidistant time steps. The input parameters are equatorial coordinates α and δ, distance d from the sun, heliocentric radial velocity v_{rad} and observed absolute proper motions $\mu_\alpha \cos(\delta)$ and μ_δ. The tables 1, 3 and 4 contain all necessary informations. Output parameters are among others the time of flight T_{flight} it takes to travel back to the Galactic disk, crossing coordinates x_{cross} and y_{cross}, i.e. the position where the stars' trajectories intersect the disk and corresponding velocities v_x, v_y and v_z. For convenience right-handed galactocentric coordinates x, y and z are used, whereby x goes in antisolar direction and z points to the Galactic north pole, see figure 4:

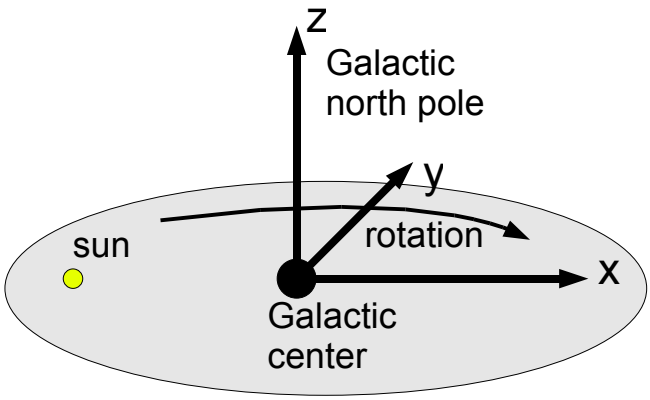

Figure 4: Galactocentric coordinate system: a right-handed frame of reference with the Galactic center at the origin. The sun's position is $x = -8.5$ kpc, $y = z = 0$.

In order to have expressive results, error estimation is indispensable. However, this is a rather strenuous task since so much sources of error occur during the whole calculation and lots of data taken from literature do not even contain any information about the limits of validity leading to further uncertainty. Moreover, straightforward error propagation is far too complex due to the use of numerical integration. Nevertheless crude estimations of error margins are achieved by taking into consideration the most significant sources:

- Experience shows that deviations in the surface gravity g dominate all other quantities when calculating the distance d according to equation 2.5. Hence a rather large error of $\Delta \log\left(\frac{g}{\text{cms}^{-2}}\right) = 0.2$ is applied, intended to compensate for the unknown and hence neglected errors of the other quantities. Therefore $d_{\min}$ and $d_{\max}$ correspond to $\log\left(\frac{g}{\text{cms}^{-2}}\right) \pm 0.2$.
- Uncertainties in the proper motions $\mu_\alpha \cdot \cos(\delta)$ and μ_δ are maintained by a weighted average over several catalogs, see table 4, and usual error estimation.
- Since literature provides error estimates for v_{rad} and inaccuracies in right ascension and declination are negligible, all input parameters for the numerical program are taken into account. So error propagation can be achieved by the following Monte Carlo method: after generating a large sample of different initial conditions assuming a Gaussian distribution for the input parameters (using the given data as mean value and standard deviation), the program computes the output parameters for each starting condition and calculates from that the statistical properties of the resulting sample such as standard deviation and mean value. Note that all input parameters are varied simultaneously.

The next section shows the necessity of proper error estimation for the interpretation of the results.

5 Results and discussion

All calculations are performed using a time step of 0.01 Myr and 5000 Monte Carlo runs. Results are summarized in tables 5 and 6 of appendix B and discussed in the following lines.

HIP 60350: Due to its extreme high current velocity $v = \sqrt{{v_\alpha}^2 + {v_\delta}^2 + {v_{\text{rad}}}^2} = 430 \pm 90$ km/s be-

ing very close to the Galactic escape speed, HIP 60350 is the most interesting star investigated in this work. It intersected the Galactic disk at $x_{\text{cross}} = -0.04 \pm 2.80$ kpc and $y_{\text{cross}} = -7 \pm 2$ kpc about $T_{\text{flight}} = 20 \pm 4$ Myr ago. This agrees to similar calculations done by Tenjes et al. (see [16]).

Knowing a good model for the Galactic rotation curve (see e.g. [1]) and hence the distance–depending rotation velocity one can compute the region of the Galaxy to which the crossing area has evolved during the star's time of flight. This allows to examine the possible places of birth of the analyzed stars. In this work, the task is to find open clusters in those regions in order to argue for or against the second creation mechanism mentioned in the introduction: close dynamical encounters in dense star clusters. The search is restricted to open clusters since their ages correspond to the ones of the investigated stars and because they are most likely found in the Galactic disk.

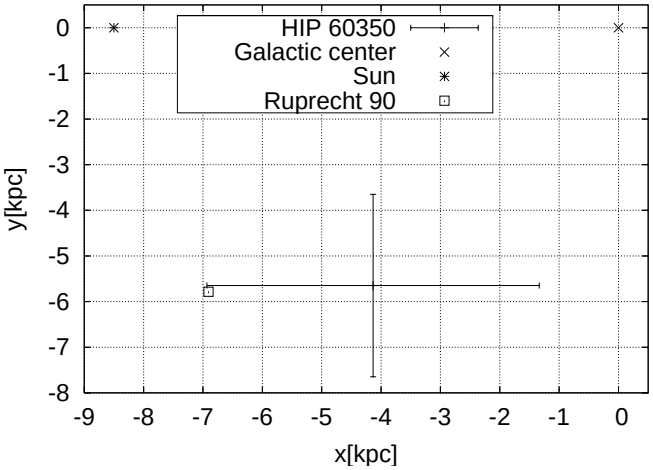

Figure 5: Open cluster candidates for HIP 60350: Ruprecht 90 is approximately 12.6 Myr old and has a z–component of -20.9 pc. For simplicity, the error margins are adopted from the crossing positions and hence are crude estimations as rotation effects are completely neglected.

For HIP 60350 only one candidate – Ruprecht 90 (age: 12.6 Myr, $z = -20.9$ pc) – is found in the WEBDA database of stellar clusters[2], compare figure 5. However, there are two serious arguments against Ruprecht 90 as birthplace of HIP 60350: firstly there is a non negligible discrepancy between the time of flight $T_{\text{flight}} = 20 \pm 4$ Myr and the cluster's age of 12.6 Myr implying that HIP 60350 began its voyage before Ruprecht 90 existed. Secondly the error margins in figure 5 (and in all following ones) are just crude estimations since they are adopted from the crossing positions neglecting completely rotational effects that would transform them in a non trivial manner. As Ruprecht 90 already lies at the outermost part of the uncertainty region, it is likely that it falls out due to the transformation.

On the other hand the first creation mechanism described in the introduction, the supernova scenario, is according to [16] also unlikely because of the huge relative ejection velocity $v_{\text{ej}} = \sqrt{{v_r}^2 + (v_\varphi - v_{\text{rot}})^2 + {v_z}^2} = 440 \pm 230$ km/s (see table 6 for values and descriptions).

Therefore the origin of HIP 60350 remains still uncertain. Tenjes et al. assume that an open cluster of appropriate age exists in the crossing region being yet undiscovered due to absorption in the interstellar medium and propose more precise spectroscopic and kinematic measurements to bring some light into the dark.

PG 0934+145: With a time of flight $T_{\text{flight}} = 27 \pm 6$ Myr being much smaller than the age of 61 Myr PG 0934+145 could come without problems from the Galactic disk. Moreover abundance estimates achieved in [14] do not differ significantly from those belonging to stars of the Galactic plane. Nevertheless not even one open cluster candidate is found for PG 0934+241. The small absolute circular velocity $v_\varphi = 30 \pm 50$ km/s of PG 0934+145 implies an ejection velocity directed strongly against the Galactic rotation.

Feige 40: For Feige 40 at least four open cluster candidates exist: ASCC 109 (204 Myr, 27.6 pc),

[2] see http://www.univie.ac.at/webda/ for more information

NGC 7058 (224 Myr, 4.1 pc), ASCC 103 (234 Myr, 88.0 pc) and Alessi 20 (166 Myr, −29.0 pc). The first two seem to be the best ones since their ages fit to that of Feige 40 which is $T_{\text{evol}} = 200$ Myr. Furthermore their spatial distance is not so far, see figure 6.

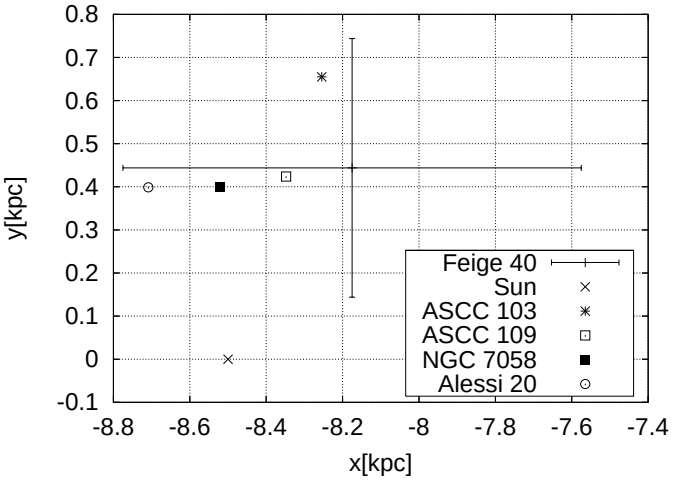

Figure 6: Open cluster candidates for Feige 40: ASCC 109 (204 Myr, 27.6 pc) and NGC 7058 (224 Myr, 4.1 pc) seem to be perfect possible places of birth for Feige 40 due to their age and small z-component. But ASCC 103 (234 Myr, 88.0 pc) and Alessi 20 (166 Myr, −29.0 pc) cannot be disdained as well.

Apart from the discrepancy between the time of flight $T_{\text{flight}} = 15 \pm 4$ Myr and age indicating that Feige 40 was ejected a long time after the cluster began to exist, the probability for one of the mentioned clusters to be the birthplace of Feige 40 is large.

PG 1205+228: Rolleston et al. state that PG 1205+228 is most certainly a Galactic disk run-away (see [14]). Comparing evolution age $T_{\text{evol}} = 51$ Myr to $T_{\text{flight}} = 15 \pm 2$ Myr this assumption can be assured. Yet no open clusters are found to match the crossing region of PG 1205+228.

PG 1315-077: According to Hambly et al. ([3]) PG 1315-077 probably originated in the halo and not in the Galactic disk. However, the huge uncertainty in the stellar age leaves space for a wide range of interpretations. Comparing $T_{\text{flight}} = 22 \pm 5$ Myr to $T_{\text{evol}} = 1 \ldots 20$ Myr a run-away scenario cannot be excluded. Moreover there even exists a possible birthplace in the Galactic plane, the open cluster vdBergh 113 (32 Myr, −46.6 pc), see figure 7.

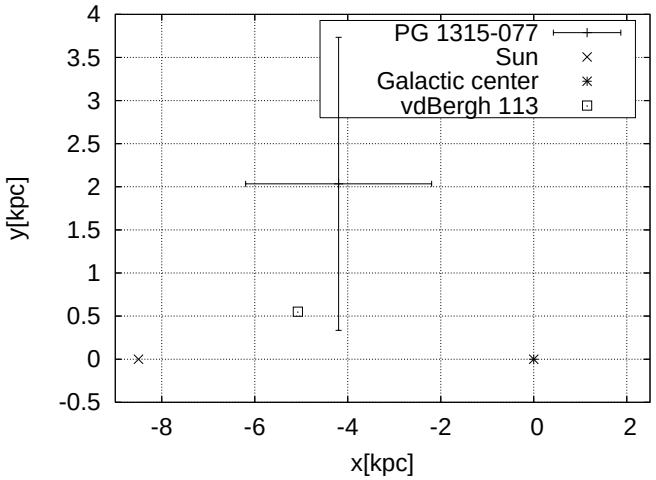

Figure 7: Open cluster candidates for PG 1315-077: vdBergh 113 is 32 Myr old and has $z = -46.6$ pc.

Unfortunately, the lifetime of vdBergh 113 exceeds the evolution age of PG 1315-077 by far, which should not be the case. But as the latter one is not determined accurately, this problem could be solved by precise further measurements.

PHL 159 and **BD -15 115**: PHL 159 and BD -15 115 have times of flight almost identical to their lifetimes indicating that they could come from the Galactic disk if they were ejected very soon after formation in accordance with the results of Ramspeck et al. ([13]). Unfortunately no corresponding open clusters are listed in the WEBDA database.

PHL 346: Similar to Ramspeck et al. ([13]) the time of flight $T_{\text{flight}} = 29 \pm 21$ Myr of PHL 346 is larger than the evolution age $T_{\text{evol}} = 19 \pm 2$ Myr arguing for a formation in the halo and against the run-away scenario. Furthermore, there is no appropriate open cluster fitting to PHL 346 and the huge relative ejection velocity

$v_{\rm ej} = \sqrt{{v_r}^2 + (v_\varphi - v_{\rm rot})^2 + {v_z}^2} = 460 \pm 80$ km/s almost excludes the supernova scenario. Perhaps PHL 346 is not a run-away star from the Galactic disk at all.

PG 2345+241: PG 2345+241 is possibly a run-away star coming from an open star cluster of the Galactic plane as several good cluster candidates exist: Biurakan 1 (17.8 Myr, 49.1 pc), NGC 7128 (17.9 Myr, 17.3 pc) and NGC 7419 (19.2 Myr, 27.0 pc) coincide in their ages quite well to the lifetime $T_{\rm evol} = 19$ Myr of PG 2345+241. Berkeley 62 (15.3 Myr, 35.2 pc), NGC 0581 (21.7 Myr, −69.1 pc) and NGC 0663 (16.2 Myr, −32.1 pc) are spatially close to PG 2345+241, see figure 8.

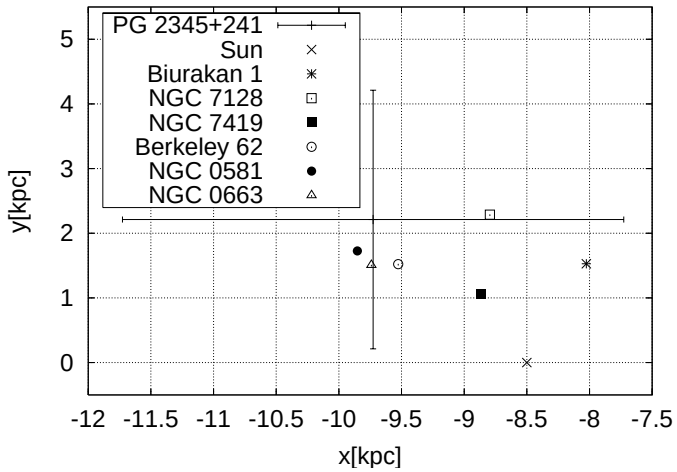

Figure 8: Open cluster candidates for PG 2345+241: Biurakan 1 (17.8 Myr, 49.1 pc), NGC 7128 (17.9 Myr, 17.3 pc) and NGC 7419 (19.2 Myr, 27.0 pc) have matching lifetimes, Berkeley 62 (15.3 Myr, 35.2 pc), NGC 0581 (21.7 Myr, −69.1 pc) and NGC 0663 (16.2 Myr, −32.1 pc) are spatially close to PG 2345+241.

What is more, the time of flight $T_{\rm flight} = 24 \pm 14$ Myr is not directly in contradiction to this conclusion.

HD 149363: For HD 149363 three open cluster candidates are found: Bochum 14 (9.9 Myr, −5.0 pc), NGC 6683 (10 Myr, −16.5 pc) and Biurakan 2 (10.3 Myr, 26.0 pc). Despite agreeing very well with the age $T_{\rm evol} = 10$ Myr of HD 149363, their location at the edge of the (crude estimated) uncertainty region causes serious doubts about their qualification as birthplace of HD 149363, see figure 9. A more detailed error analysis could dissipate these doubts, especially as $T_{\rm flight} = 7 \pm 7$ Myr matches the star's age being in favor of a run-away scenario.

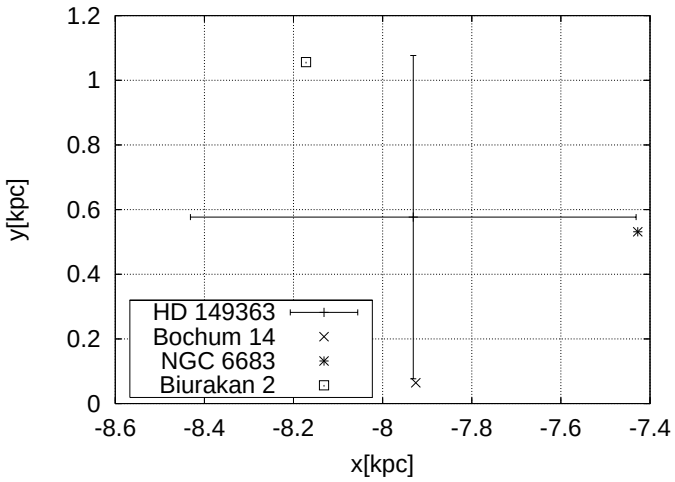

Figure 9: Open cluster candidates for HD 149363: The large spatial distance in comparison to error margins decreases the probability for Bochum 14, NGC 6683 and Biurakan 2 to be the birthplace of HD 149363.

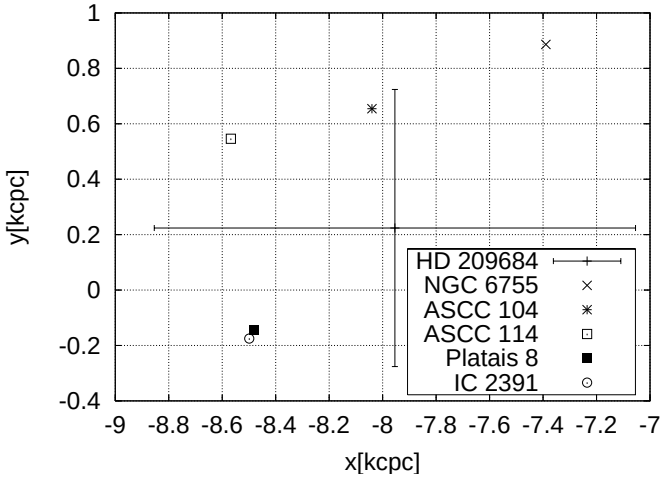

Figure 10: Open cluster candidates for HD 209684: NGC 6755 (52.3 Myr, −41.9 pc), ASCC 104 (51.3 Myr, −21.6 pc), ASCC 114 (56.2 Myr, 9.6 pc), Platais 8 (56.2 Myr, −20.3 pc) and IC 2391 (45.8 Myr, −20.8 pc).

HD 209684: Similar story as for HD 149363: Several cluster candidates are found – NGC 6755 (52.3 Myr, −41.9 pc), ASCC 104 (51.3 Myr, −21.6 pc), ASCC 114 (56.2 Myr, 9.6 pc), Platais 8 (56.2 Myr, −20.3 pc) and IC 2391 (45.8 Myr, −20.8 pc) – having appropriate ages around $T_{\mathrm{evol}} = 50$ Myr but less fitting positions, see figure 10. Remarkable about HD 209684 is the small relative ejection velocity $v_{\mathrm{ej}} = \sqrt{{v_r}^2 + (v_\varphi - v_{\mathrm{rot}})^2 + {v_z}^2} = 100 \pm 25$ km/s possibly preferring the supernova scenario.

6 Summary

In this project, eleven run-away stars are analyzed with the help of their kinematic properties.

A brief discussion about the definition and creation mechanism of run-away stars in the introduction is followed by the determination of the three dimensional velocities of each stellar body. In order to do so, distances have to be calculated from spectroscopic quantities m_{V}, T_{eff}, $\log\left(\frac{g}{\mathrm{cms}^{-2}}\right)$ and M, provided by literature. Taking proper motions from astronomical catalogs and radial velocities from spectroscopy, all velocity components are known.

In the subsequent sections, the applied model for the Galactic gravitational potential by Allen & Santillán as well as the numerical program are described, completed by deliberations about error estimation.

In the last but one section, results are presented and discussed: HIP 60350 seems to have originated in a not yet discovered star cluster of the Galactic disk. Feige 40, PG 1315-077, PG 2345+241, HD 149363 and HD 209684 have been more or less likely created by close dynamical encounters in open clusters. Possible candidates are stated. With a time of flight being unambiguously larger than its age, perhaps PHL 346 is not a runaway at all. The remaining stars show clear hints to come from the Galactic disk, however, no open cluster candidates are found for them. Reasons for that are manifold:

- not all clusters might have been discovered until now
- other ejection mechanisms such as the supernova scenario are possible
- initial positions and velocities are not known exact enough so that numerical calculations could lead to wrong crossing regions

The results are summarized in compact form in appendix B.

Acknowledgements

Thanks goes to Uli Heber for offering this interesting project and for spending a lot of time to give helpful pieces of advice. Moreover this project has made use of the WEBDA database, operated at the Institute for Astronomy of the University of Vienna.

A Stellar data

Table 3: Spectroscopic data of examined stars

star	m_V	T_{eff} [K]	$\log\left(\frac{g}{\text{cms}^{-2}}\right)$	v_{rad} [km/s]	M [$M_\odot$]	T_{evol} [Myr]	reference
HIP 60350	11.60	16400	4.0	223 ± 15	5	15	[2],[7]
PG 0934+145	13.14	16600	4.0	105 ± 4	5.3	61	[14]
Feige 40	11.1	15500	4.5	71.5 ± 5.7	3.9	200	[8],[9]
PG 1205+228	11.01	16600	4.1	156 ± 4	5.1	51	[14]
PG 1315-077	12.32	19000	4.3	134 ± 5	6.0	$1 \ldots 20$	[3]
PHL 159	10.9	18500	3.59	88 ± 3	8.0	28 ± 2	[13]
PHL 346	11.4	20700	3.58	63 ± 4	9.9	19±2	[13]
BD -15 115	10.8	20100	3.81	93 ± 4	8.0	26±4	[13]
PG 2345+241	12.43	18800	4.2	82 ± 3	6.0	19	[14]
HD 149363	7.8	30000	4.0	145.8 ± 7.1	15	10	[8], [9]
HD 209684	9.8	21000	4.25	71.6 ± 7.7	6.8	50	[8], [9]

Table 4: Kinematic data of investigated stars: proper motions are obtained by averaging over the given catalogs, whereby "Hipparcos (van Leeuwen 2007)" (1), "UCAC2 (Zacharias et al. 2003)" (2), "USNO-B1 (Monet et al. 2003)" (3) and "Carlsberg Meridian Catalog (CMC 1999)" (4) are weighted twice as much as "ASCC (Kharchenko 2001)" (5), "Tycho-2 (Hog et al. 2000)" (6) and "ACT (Urban et al. 1997)" (7).

star	α [h,m,s]	δ [°,am,as]	$\mu_\alpha \cdot \cos(\delta)$ [mas/yr]	μ_δ [mas/yr]	catalogs used
HIP 60350	12 22 29.6	+40 49 36	-14 ± 2	16.4 ± 0.3	1, 2, 3, 4, 5, 6, 7
PG 0934+145	09 37 04.0	+14 18 24	7 ± 3	-4 ± 3	2
Feige 40	11 21 29.3	+11 19 17	-1 ± 2	-7 ± 2	1, 2, 3, 4, 5, 6, 7
PG 1205+228	12 07 57.7	+22 31 51	-16 ± 2	-0.6 ± 0.9	1, 2, 3, 5, 6, 7
PG 1315-077	13 17 37.1	-07 57 47	-8 ± 7	-2 ± 3	2
PHL 159	21 48 42	+01 57 00	-3 ± 2	-9 ± 1	1, 2, 3, 5, 6, 7
PHL 346	22 37 38.3	-18 39 51	5 ± 2	-7.7 ± 0.9	2, 3, 5, 6, 7
BD -15 115	00 38 20.3	-14 59 54	8 ± 2	0.2 ± 0.6	1, 2, 3, 5, 6, 7
PG 2229+099	22 32 08.5	+10 14 25	-7 ± 2	-3.3 ± 0.5	2, 4, 5
PG 2345+241	23 48 22.4	+24 23 06	-2 ± 2	-4 ± 2	2, 3, 5, 6, 7
HD 149363	16 34 28.3	-06 08 10	-9 ± 1	-14 ± 2	2, 4, 5
HD 209684	22 05 31.2	-13 46 12	0 ± 2	-1.0 ± 0.6	2, 3, 4, 5, 6

B Results

Table 5: Crossing coordinates x_{cross} and y_{cross} and times of flight T_{flight} for analyzed stars maintained from the intersection of the stars' orbits with the Galactic plane. For comparison, the corresponding stellar ages T_{evol} are stated as well.

star	x_{cross}[kpc]	y_{cross}[kpc]	T_{evol}[Myr]	T_{flight}[Myr]
HIP 60350	-0.04 ± 2.80	-7 ± 2	15	20 ± 4
PG 0934+145	-14.6 ± 3.1	-4.5 ± 1.9	61	27 ± 6
Feige 40	-7.7 ± 0.6	-2.8 ± 0.3	200	15 ± 4
PG 1205+228	-5.1 ± 0.7	-2.0 ± 0.2	51	15 ± 2
PG 1315-077	-4 ± 2	-2.4 ± 1.7	$1 \ldots 20$	22 ± 5
PHL 159	-10 ± 2	0 ± 1	28 ± 2	25 ± 18
PHL 346	-3 ± 2	5 ± 2	19 ± 2	29 ± 21
BD -15 115	-2 ± 1	-3.4 ± 0.7	26 ± 4	28 ± 2
PG 2345+241	-10 ± 2	-3 ± 2	19	24 ± 14
HD 149363	-7.9 ± 0.5	-0.9 ± 0.5	10	7 ± 7
HD 209684	-7.1 ± 0.9	-3.6 ± 0.5	50	18 ± 6

Table 6: Absolute ejection velocities v_x, v_y, and v_z for examined stars, defined as velocity components at the moment of disk intersection. Additionally $v_r = v_x \cdot \cos(\pi - \varphi) + v_y \cdot \sin(\pi - \varphi)$, $v_\varphi = v_x \cdot \sin(\pi - \varphi) - v_y \cdot \cos(\pi - \varphi)$ and $v_\varphi - v_{\text{rot}}$ are given, whereby r and φ are two dimensional galactocentric polar coordinates with φ increasing in direction of Galactic rotation and $\varphi = 0$ for solar orientation (see figure 4). Hence $v_\varphi - v_{\text{rot}}$ is the ejection velocity in angular direction corrected for Galactic rotation.

star	v_x[km/s]	v_y[km/s]	v_z[km/s]	v_r[km/s]	v_φ[km/s]	$v_\varphi - v_{\text{rot}}$[km/s]
HIP 60350	-450 ± 50	310 ± 20	210 ± 20	-310 ± 220	450 ± 120	230 ± 130
PG 0934+145	90 ± 90	60 ± 70	210 ± 70	-110 ± 100	30 ± 50	-200 ± 60
Feige 40	-70 ± 20	140 ± 20	90 ± 20	20 ± 20	160 ± 10	-60 ± 20
PG 1205+228	-260 ± 40	90 ± 20	180 ± 10	210 ± 50	180 ± 40	-45 ± 50
PG 1315-077	-180 ± 110	0 ± 70	210 ± 40	150 ± 150	90 ± 130	-120 ± 140
PHL 159	110 ± 40	150 ± 40	-160 ± 40	-110 ± 40	150 ± 10	-70 ± 20
PHL 346	-100 ± 50	-10 ± 50	-330 ± 50	40 ± 60	-90 ± 80	-315 ± 50
BD -15 115	-290 ± 40	90 ± 30	-220 ± 30	70 ± 90	290 ± 40	80 ± 50
PG 2345+241	-30 ± 50	270 ± 30	-140 ± 30	-50 ± 50	270 ± 20	50 ± 20
HD 149363	110 ± 30	160 ± 30	80 ± 20	-130 ± 30	150 ± 10	-70 ± 20
HD 209684	-60 ± 10	230 ± 30	-90 ± 20	-50 ± 10	230 ± 10	10 ± 20

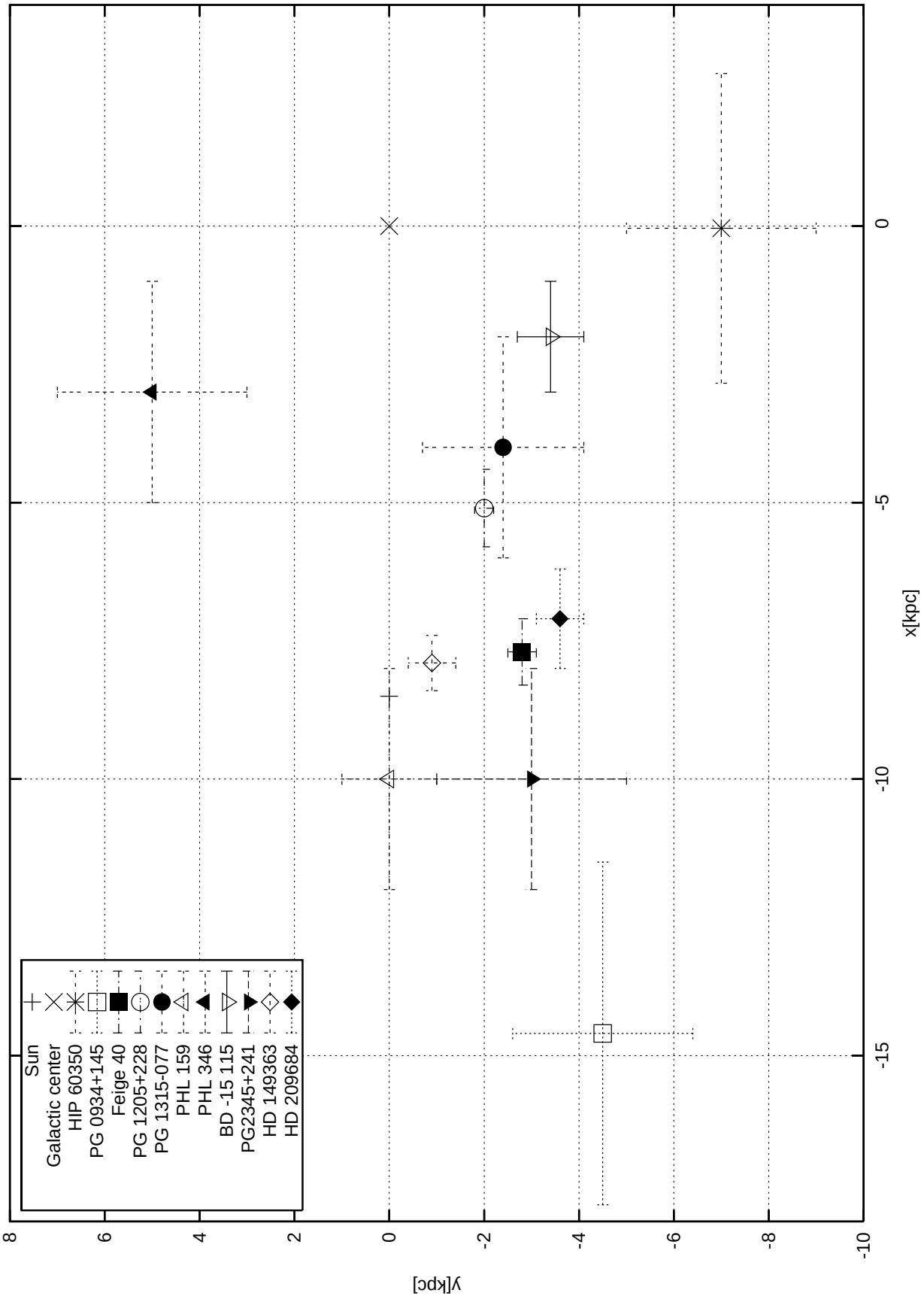

Figure 11: Crossing coordinates for all investigated stars: the data come from table 5.

References

[1] Allen C., Santillán A., *An improved model of the Galactic mass distribution for orbit computations*, 1991, RMxAA, 22, 255-263

[2] De Boer K. S., Heber U., Richtler T., *The nature of the four blue halo stars of Tobin*, 1988, A&A, 202, 113-116

[3] Hambly N. C., Conlon E. S., Dufton P. L., Keenan F. P., Little J. E., *Model atmosphere and kinematical analyses of early-type, high galactic latitude stellar candidates from the UKST UBVRI survey*, 1993, ApJ, 417, 706-712

[4] Heber U., Edelmann H., Napitwotzki R., Altmann M., Scholz R.-D., *The B-type giant HD 271791 in the Galactic halo – linking run-away stars to hyper-velocity stars*, 2008, A&A, 483, L21-L24

[5] Hills J. G., *Hyper-velocity and tidal stars from binaries disrupted by a massive Galactic black hole*, 1988, Nature, 331, 687-689

[6] Kurucz R. L., *Model Atmospheres for G, F, A, B and O Stars*, 1979, ApJ Supplement Series, 40, 1-340

[7] Maitzen H. M., Paunzen E., Pressberger R., Slettebak A., Wagner R.M., *HIP 60350: an extreme runaway star*, 1998, A&A, 339, 782-786

[8] Martin J. C., *The origins and evolutionary status of B stars found far from the Galactic plane. I. Composition and spectral features*, 2004, AJ, 128, 2474-2500

[9] Martin J. C., *The origins and evolutionary status of B stars found far from the galactic plane. II. Kinematics and full sample analysis*, 2006, AJ, 131, 3047-3068

[10] Moore P., Robinson L. J., *Philip's Astronomy Encyclopedia* (Octopus Publishing Group, 2002)

[11] Murdin P., *Encyclopedia of Astronomy and Astrophysics* (Nature Publishing Group, 2001)

[12] Odenkirchen M., Brosche P., *Orbits of galactic globular clusters*, 1992, AN, 313, 69

[13] Ramspeck M., Heber U., Moehler S., *Early type stars at high galactic latitudes – I. Ten young massive B-type stars*, 2001, A&A, 378, 907-917

[14] Rolleston W. R. J., Hambly N. C., Keenan F. P., Dufton P. L., Saffer R. A., *Early-type stars in the Galactic halo from the Palomar-Green Survey – II: A sample of distant, apparently young Population I stars*, 1999, A&A, 347, 69-76

[15] Schaller G., Schaerer D., Meynet G., Maeder A., *New grids of stellar models from 0.8 to 120 solar masses at Z=0.020 and Z=0.001*, 1992, A&AS, 96, 269-331

[16] Tenjes P., Einasto J., Maitzen H. M., Zinnecker H., *Origin and possible birthplace of the extreme runaway star HIP 60350*, 2001, A&A, 369, 530-536